

# Intra-Cavity Adaptive Optics Control of Lasers

W. Lubeigt, G.J. Valentine and D. Burns  
Institute of Photonics, University of Strathclyde,  
106 Rottenrow, Glasgow, G4 0NW

## Abstract

*A computer-controlled, self-optimisation, adaptive optics system has been used to control the performance of a solid-state laser. The control program has been upgraded to use mixed algorithms and has been optimised for speed. Transient optimisation has also been investigated to reduce the fluctuation of the brightness at the laser turn-on*

Keywords: Solid-state laser, spatial mode, thermal effects, adaptive optics

## Introduction

Thermally induced aberrations are one of the main impediments to be overcome in developing high-power solid-state lasers [1]. These aberrations, induced by the substantial heat loading, can severely limit the transverse mode quality in high average power laser systems [2]. Unfortunately, there is no simple, effective means of compensating against the effects of the non-spherical component of the induced thermal lens. The goal of this work was to investigate the potential of using intra-cavity adaptive optics techniques as a general technique for thermal aberration correction over a wide operating range, and so, extending the potential of high power solid state lasers.

An account of our earlier work [3] described the development of a computer-controlled, self-optimisation, adaptive optics feedback system to enhance the brightness of various test-bed lasers. The control loop derived is shown in figure 1 and consisted of:

- a grazing incidence laser featuring an intra-cavity deformable membrane mirror (DMM)
- a beam quality sensor to determine the laser performance, or 'fitness value'
- a personal computer hosting the control software based around an optimisation algorithm that searches for the optimal shape of the intra-cavity deformable membrane

mirror (DMM)

- a high voltage, multi-channel digital to analog conversion unit to interface the laser to the optimisation scheme

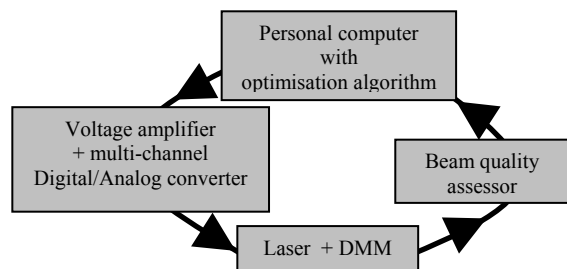


**Figure 1** Closed loop intra-cavity adaptive optics optimisation scheme

A complete description of these elements was given in [3], however, further improvements to the control network were performed during this year's work and these will be summarised below.

Another potential area for the exploitation of adaptive optics control of lasers is during the transient phase immediately following turn-on of the laser. Here, the DMM can be used to reduce the time for the laser to reach both its maximum power level and full brightness. As this investigation required a stable laser system, a new laser test-bed was configured based around a commercial CEO Nd:YLF laser module.

In this paper, we describe the developments in the control software necessary to fully exploit adaptive laser control. In section 2, a description of the new laser system is given followed by a discussion of our transient control investigations.

### Control software development

Several modifications were made to the software that controls the progress of the laser optimisation.

Firstly, in the laser cavity, the aberrations to be compensated can be considered as the addition of a basic aberration set such as the first-order thermal lens, spherical aberration, astigmatism, coma etc. So, in order to better suit this, the optimisation process was divided into two optimisation stages: an initial ‘coarse’ stage followed by a final ‘refinement’ stage. The coarse optimisation stage finds the mirror shape which then defines the start point of the refinement optimisation. To implement this, both stages were developed and integrated within the software. In the coarse stage, all actuators of each of the four concentric actuator rings were grouped in order to enable the algorithm to run with only four ‘super actuators’. This coarse optimisation imposes only a small computational overhead since the search field has now only  $256^4$  possible combinations. In addition, an option was introduced where the algorithms can operate around the starting mirror shape within a pre-set voltage range. This configuration enables a smaller search field optimisation search and avoids the situation when large optical changes cause the collapse of the transverse mode of the laser output [3].

In addition, the Modified Hill-Climbing (MHC) algorithm was re-written and inserted into the control interface. Several of its parameters, such as the number of cycles, the size of the search space and the step size were made reconfigurable. The MHC can also be implemented after a Genetic Algorithm (GA) search in order to enable a two-stage optimisation search

process. In this way, a significant reduction in the duration of a GA-based optimisation was possible.

The user interface of the control program was also considerably simplified to make it more ‘user-friendly’.

### New Nd:YLF laser cavity

The grazing-incidence was deemed too unstable for the transient optimisation to be performed. Another laser cavity was therefore built around a Nd:YLF module from Cutting Edge Optronics. It consists of a 63mm long and 3mm diameter Nd:YLF rod evenly pumped by a set of nine diode laser arrays. When installed in a basic 2-mirror laser cavity 25W highly multimode oscillation resulted, as shown in figure 2.

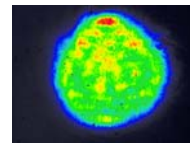


**Figure 2** *Transverse profile of the 25W Nd:YLF laser*

As the Nd:YLF crystal is natural birefringence oscillation can occur at two different wavelengths having different polarization (1053nm for the  $\sigma$ -polarization and 1047nm for the  $\pi$ -polarization). Also, this natural birefringence effectively eliminates the thermally induced birefringence from degrading the laser performance. In our configuration, the laser was found to oscillate in the higher gain  $\pi$ -polarisation emitting at 1047nm. The gross spherical thermally induced lens was experimentally measured using a probe He-Ne laser and estimated to be  $f = -3\text{m}$  and  $f = -1\text{m}$  for the tangential and sagittal planes respectively.

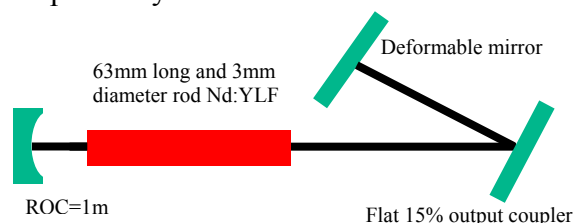


**Figure 3** *Nd:YLF laser cavity featuring the DMM*

The output beam produced from the laser cavity was highly multi transverse mode. It

was therefore decided to minimise this by using the same technique as deployed in the grazing incidence Nd:YLF laser [3], i.e. modifying the laser cavity to maximise the fundamental mode size in the gain medium. The subsequent laser cavity featuring the DMM intra-cavity (as shown in figure 3) produced 4W output power with a low order transverse spatial mode as displayed in figure 4.

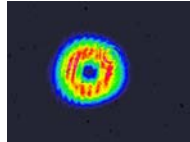


**Figure 4** Transverse intensity distribution of the laser output beam

### Transient optimisation

The aim of this study was to investigate the potential of controlling the laser output during the transient thermal regime at the ‘turn-on’ of the laser. The ‘turn-on’ time is defined here as the time taken for the laser to reach a stable output where its power and/or brightness are optimal. This point is equivalent to the time necessary for the laser to reach thermal equilibrium as described in figures 5 and 6. The objective of the investigation is therefore to force the laser to evolve to its brightest state in the minimum time,  $t_f$ , using adaptive control (see fig. 6).

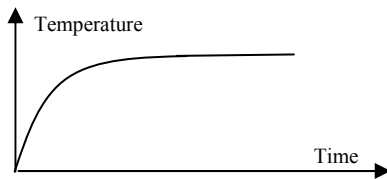


**Figure 5** Temperature profile at a point in the pumped region of the gain medium

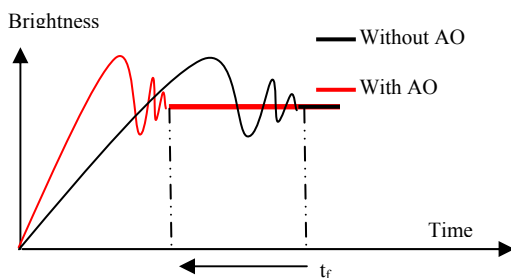


**Figure 6** Evolution of the laser brightness with and without AO control

### Optimisation strategy

For transient optimisation, it was decided to segment the thermal build-up time into several sections (or periods of  $\Delta t$  as shown in figure 7). The number of segments can be arbitrarily chosen, however, the width of each  $\Delta t$  should reflect a timescale over which thermal aberrations are minimal. The problem can now be solved by finding the optimum shape of the DMM within each segment such that the brightness is maximised. When the sequence of mirror shapes is known then they can be applied in turn at the appropriate time after laser turn-on by way of a look-up table.

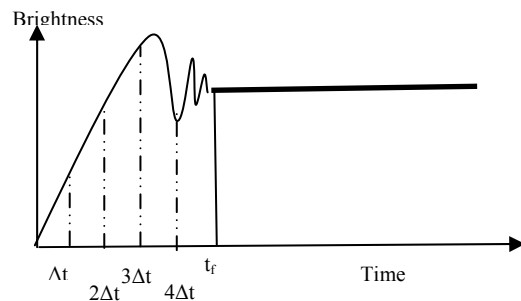


**Figure 7** Dissection of the thermal build-up time into several sequential  $\Delta t$  segments

The first step is therefore to find the adequate mirror shape for each  $\Delta t$ , and the basic algorithm for this process is described in figure 8. The starting mirror shape is first applied, the laser is turned on. After a delay of  $\Delta t$ , a mirror shape is applied according to the optimisation algorithm used, and the fitness is then instantly measured and recorded. The laser is then turned off and the process applied repeatedly until the mirror shape giving the highest brightness is obtained by the search algorithm.

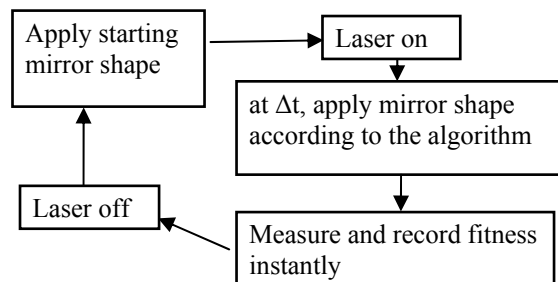


**Figure 8** Search for the adequate membrane shape for  $t=\Delta t$

A similar process is then applied to obtain the best mirror shape at  $t=2\Delta t$  (see figure 9). Here, the starting mirror shape is applied, the laser is turned on, and after a delay of  $\Delta t$ , the optimum mirror shape found earlier is applied. A process similar is then used to find the optimum mirror shape at time  $2\Delta t$ . With every repetition used to find the new optimum shape at  $2\Delta t$  the previously found optimal values are applied at the appropriate time. In this way, a table of optimal values for each segment of time is found, i.e. to find the optimal value at time  $t=n\Delta t$ , each previous optimal value must be known (and applied in turn).

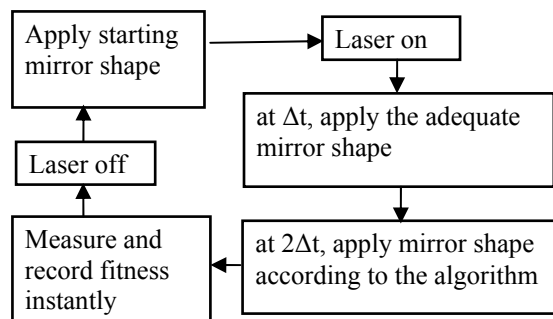


**Figure 9** Search for the adequate membrane shape for  $t=2\Delta t$

With respect to potential scenarios where transient optimisation may be relevant, two cases are obvious:

- Case 1 – directly after the pump source to the laser is switched on
- Case 2 – after an intra-cavity blocker is removed under conditions of constant pumping

Figure 10 shows the temperature build up in both cases for a point located in the pumped region of the gain medium.

#### Measurement of the thermal build-up time

The fitness was measured using a simple *power-in-a-bucket* measurement, using a  $100\mu\text{m}$  diameter pinhole and photodiode to provide the laser's operational fitness value.

A chopper was inserted in the laser cavity in order to create the necessary conditions for case 2, and the thermal build-up time was measured to be 5ms (see figure 11). The fast build-up was to be expected in this

case as the only contribution to the temperature change in the laser rod was that associated with the power extracted as useful laser output. As the output power is modest compared to the pumping power the temperature variation is small, and so, the transient associated with re-establishing thermal equilibrium is rapid.

The thermal build-up time was also measured for the case 1. The power supply to the laser module was modified in order to allow the intensity to change from no intensity to a maximum value in 24ms. The thermal build-up as measured at about 15s as shown in figure 12.

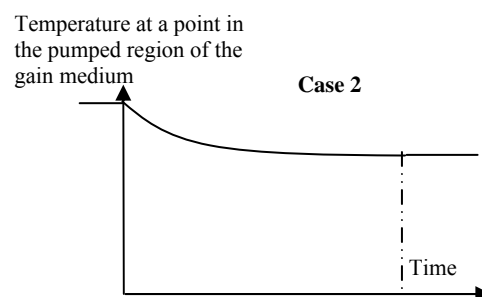
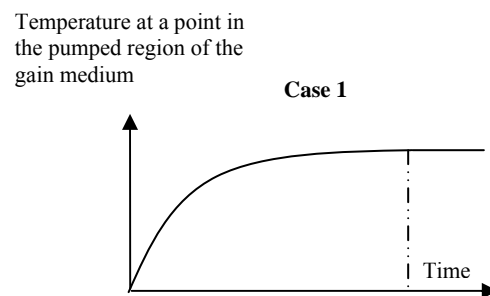


**Figure 10** Transient laser output profiles for cases 1 and 2

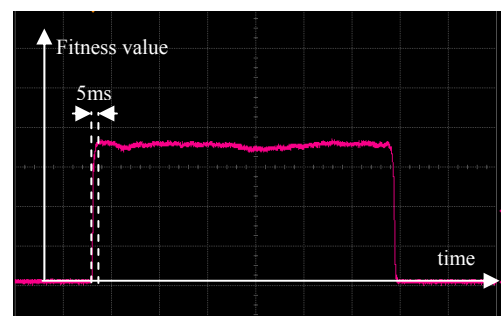


**Figure 11** Temporal evolution of the fitness value for case 2

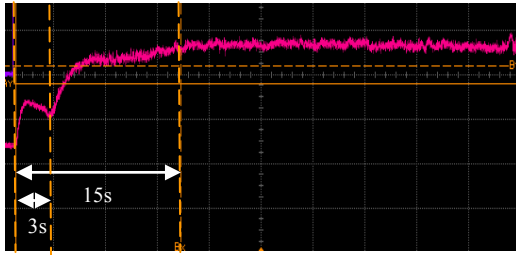


**Figure 12** Temporal evolution of the fitness value for case 1

The large thermal build-up time for case 1 can be explained by the large temperature change between the lasing (i.e. pump on) and non-lasing (pump off) state. It is noted that the transient response of the laser output associated with the thermalisation within the laser rod could vary significantly (from 4s to 15s) according to the specific pumping and alignment conditions.

#### *Reduction of the software response time*

The response of the control program i.e. the time taken for a full iteration was initially measured at 66ms. This time was effectively independent of the algorithm used. The control iteration consisted of the reading of an analog value (the output laser beam quality parameter), the algorithmic processing, and the subsequent application of the voltages to the mirror. Initial modifications were performed in order to reduce the complexity of the control program, removing all unnecessary functions other than those absolutely necessary for the transient optimisation. Specifically all graphical representations were, useful for visualisation, were reduced to a minimum. After this process, the iteration time was reduced to 55ms.

The iteration cycle was decomposed in order to identify the temporal ‘bottleneck’. The time taken to apply the voltages to the mirror was measured as 1ms, in agreement with the specified value for the deformable mirror. The USB-addressed reading of the analog value was obtained as follows: the pc sends a signal to the control unit asking for the reading, the reading is then obtained and its value is sent back to the pc. It was observed that this process was taking >30ms as the USB-port requires 15ms to

both send and receive any amount of data. It was therefore clear that accessing the analog value corresponding to the laser fitness was significantly limiting the iteration speed of the control network. Such USB addressed systems have very good speed for large blocks (or streams) of data, however, are time constrained for single data values. To circumvent this issue a parallel-port addressed single-channel ‘pico-scope’ (Pico Technology Ltd) was configured and implemented. With this component the resultant iteration time was therefore reduced to 11ms.

Even though the iteration time would allow transient optimisation studies for case 2, it was decided to concentrate on case 1 as this represents a more real-world requirement for high power/energy laser systems.

#### *Results and observation*

The initial attempts for the transient optimisation were performed on the laser cavity shown in figure 3 which had a 15s thermal build-up time. The value for  $\Delta t$  was 3s as displayed in figure 12. The frequency of the laser operation was kept at 25mHz to ensure the steady state temperature to be reached. Several optimisations were undertaken, however, only marginal improvement in the brightness value were recorded after  $\Delta t=3s$ .

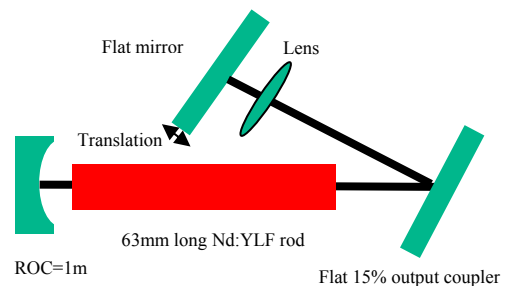


**Figure 13** Nd:YLF laser cavity featuring intra-cavity active optics

In this system the thermal lens varies from a negligible value (i.e. the laser is unpumped) to a state where the thermally induced lens has tangential and sagittal focal lengths of  $f=-3m$  and  $f=-1m$  respectively. This then leads to a considerable reconfiguration of the laser cavity, as evidenced by an ABCD matrix analysis (see later). This analysis

also makes clear that the DMM used here does not possess sufficient stroke to compensate for the induced aberrations. So, in the presence of the large thermal lens changes, associated with laser turn-on, another technique is required to maintain mode control and stability.

The ABCD matrix-based approach was used to predict the size of the fundamental mode of the cavity shown in figure 13. This laser is identical to that used previously apart from the inclusion of an intra-cavity lens. In this configuration it was observed that a translation of the end-mirror could be used to compensate for the first-order thermal lensing associated with the turn-on of our Nd:YLF laser.

With no pumping, the beam radius within the laser rod (see figure 14) is 731 $\mu\text{m}$  in both sagittal and tangential planes. Using the measured values for the thermally induced lensing, it was found that a 4mm translation of the intra-cavity lens resulted in a beam radius of 703 $\mu\text{m}$  and 755 $\mu\text{m}$  for the tangential and sagittal planes respectively (see fig. 15). The mode volume for the cold and hot cavities can therefore be made approximately equal by the lens motion. It is clear that by controlling the position of, in this example, an intra-cavity lens, that the thermal transients associated with laser turn-on should be controllable. Higher-order distortion control would then be implemented via the deformable mirror as demonstrated in our steady-state studies. Further investigations are currently underway to assess this technique.

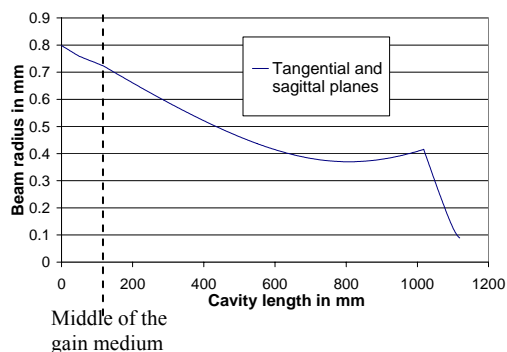


**Figure 14** Beam radius of the fundamental mode of the Nd:YLF laser cavity

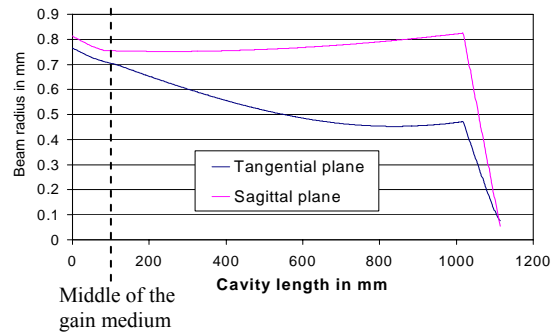


**Figure 15** Beam radius of the fundamental mode of the Nd:YLF laser cavity

## Conclusion

The work described in this report was concerned with the automatic control of a solid-state laser using an intra-cavity deformable membrane mirror. A closed-loop control system was developed to compensate for the thermally-induced lens responsible for degradation of the beam quality and efficiency of the laser output.

Further improvements and refinements were supplemented to the control software. In the algorithm procedure, the actuators of the DMM were grouped ‘super-actuators’ to affect an initial coarse stage optimisation to alleviate the issue of modal collapse. In addition, a two-stage optimisation process was configured combining the virtues of the genetic and hill-climbing algorithms. Finally, investigations on the potential for transient optimisation were also undertaken on a re-configured Nd:YLF laser. Here, the DMM was found to lack sufficient stroke to fully compensate for the variation in the thermal lensing relating to laser turn-on. It was found, however, that the use of an active optics technique should allow full temporal thermal distortion compensation.

## References

1. J.M. Eggleston, T.J. Kane, K. Kuhn, J. Unternahrer, and R.L. Byer, “The slab geometry laser. I. Theory,” *IEEE J. Quantum Electron.*, **QE-20**, pp. 289-301, 1984
2. W. Koechner, *Solid-State Laser Engineering*, 5<sup>th</sup> edition (Springer Series in Optical Sciences, 1999)

3. W. Lubeigt, G. J. Valentine and D. Burns, Paper B5, 2<sup>nd</sup> EMRS DTC Technical Conference, Edinburgh, 2005

### **Acknowledgements**

The work reported in this paper was funded by the Electro-Magnetic Remote Sensing (EMRS) Defence Technology Centre, established by the UK Ministry of Defence and run by a consortium SELEX Sensors and Airborne Systems, Thales Defence, Roke Manor Research and Filtronic.